JOURNAL OF PHYSICAL ORGANIC CHEMISTRY
J. Phys. Org. Chem. 2000; **13:** 300–305

The RNA molecular wire: the pH-dependent change of the electronic character of adenin-9-yl is transmitted to drive the sugar and phosphate torsions in adenosine 3′, 5′-bisphosphate

Irina Velikian, Parag Acharya, Anna Trifonova, András Földesi and Jyoti Chattopadhyaya*

Department of Bioorganic Chemistry, Box 581, Biomedical Centre, University of Uppsala, S-751 23 Uppsala, Sweden

Received 26 October 1999

epoc ABSTRACT: The change of the electronic character of adenin-9-yl in adenosine 3′,5′-bisphosphate (EtpApMe, 1) in the neutral versus protonated form, in contrast to its abasic counterpart [Etp(apurinic)pMe, 2], is transmitted to modulate the sugar conformation by an interplay of stereoelectronic anomeric and *gauche* effects, which in turn dictate the phosphate conformation by tuning the 3′-O—P—O(ester) anomeric effect. It was found that with the change of protonation ⇌ deprotonation equilibrium the electronic character of the aglycone changes, which is evident from the change of the pD-dependent chemical shift of the aromatic protons (δH2 and δH8). This change in chemical shift (δH2, δH8) is linearly correlated with the pD-dependent change of $\Delta G°$ of the N ⇌ S pseudorotational equilibrium of the sugar moiety (from -2.8 kJ mol^{-1} at pD 7.9 to -1.7 kJ mol^{-1} at pD 1.0), as well as with the pD-dependent change of $\Delta G°$ of the two-state $\varepsilon^{t} \rightleftharpoons \varepsilon^{-}$ equilibrium along the phosphate backbone (from -1.9 kJ mol^{-1} at pD 7.9 to -1.5 kJ mol^{-1} at pD 1.0). Finally, the pD-dependent change of $\Delta G°$ of the N ⇌ S pseudorotational equilibrium is also linearly correlated with that of the pD-dependent $\varepsilon^{t} \rightleftharpoons \varepsilon^{-}$ equilibrium, thereby unequivocally showing that the pD-dependent change of the electronic character of adenin-9-yl moiety (to its protonated form) is indeed propogated to drive the constituent sugar and phosphate backbone conformations in a concerted manner. The absence of such a correlation in the apurinic phosphodiester 2 implies that the change of the sugar conformation in 1 is independent of the electronic character of the phosphate. This tunable one-way stereoelectronic transmission is modulated intramolecularly by a cascade of orbital overlaps basing on the donor and acceptor properties of various bonding, non-bonding and antibonding orbitals, which cause a single-stranded RNA to behave as molecular wire. Copyright © 2000 John Wiley & Sons, Ltd.

KEYWORDS: NMR conformation; adenosine 3′,5′-bisphosphate; protonation; RNA; anomeric and *gauche* effects

INTRODUCTION

The cooperativity of the three essential components of DNA and RNA, the pentofuranose, nucleobase and phosphodiester units, gives the intrinsic dynamic and architectural flexibility of nucleic acids[1a,] which manifests itself into specific biological functions. The interplay of stereoelectronic gauche[2a,d–g,l,m] and anomeric effects[2b,j,l,m,o,p] energetically drive the two-state North-type (N, *C2′-exo-C3′-endo*) ⇌ South-type (S, *C3′-exo-C2′-endo*) pseudorotational equilibrium[1a2cdci3] (Ref. 3a, pp. 27–29 for the two-state N ⇌ S pseudorotational equilibrium model and references 241–246 cited in this monograph; see pp. 5–23 of this monograph for the anomeric and *Gauche* effects) (Fig. 1). A detailed dissection[2] of various *gauche* and anomeric forces has shown that the electronic nature of various pentose sugar substituents dictates its overall conformation. The chemical nature of many of these sugar substitutents (*i.e.* the aglycone, the phosphate backbone, and the 2′/4′-substitutents) can be altered and tuned by the pH of the medium as well as by complexation with an appropriate ligand present in the solution[14].

We report here our studies on the pD-dependent conformational analysis [2–oq,13,14] of adenosine 3′,5′-bisphosphate [EtpApMe) (**1**)], which serves as a model trinucleoside diphosphate[13] mimicking the central nucleotide moiety in a single-stranded RNA. A complete interdependence of conformational preference of the sugar N ⇌ S pseudorotational1a[2] and the 3′-phosphate ε^{t} ⇌ ε^{-} equilibrium[1a,2o] in EtpApMe (**1**) has been found with the change of the protonation ⇌ deprotonation equilibrium at the N1[2o] of adenin-9-yl in **1** as a function

**Correspondence to:* J. Chattopadhyaya, Department of Biochemistry, Box 581, Biomedical Centre, University of Uppsala, S-751 23 Uppsala, Sweden.
E-mail: jyoti@bioorgchem.uu.se
Contract/grant sponsor: Swedish Board for Technical Development (TFR).
Contract/grant sponsor: Swedish Natural Science Research (NFR) Council.
Contract/grant sponsor: Swedish Board for Technical Development (NUTEK).

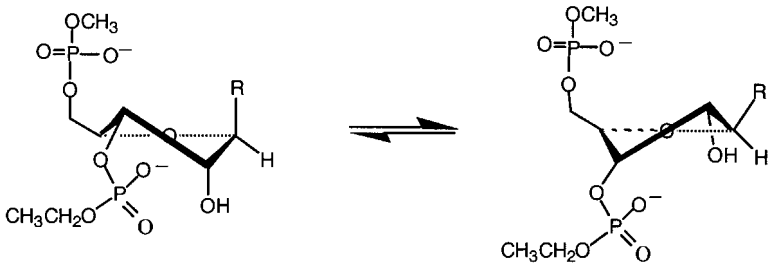

North sugar (C_3-*endo*-C_2-*exo*)
Phase angle (P) = 0° Š P Š 36°;
Puckering amplitude (Ψ_m) = 38.6° ± 3°

South sugar (C_2-*endo*-C_3-*exo*)
Phase angle (P) = 144° Š P Š 190°;
Puckering amplitude (Ψ_m) = 38.6° ± 3°

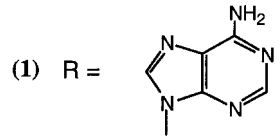

(1) R =

(2) R = H

Figure 1. The dynamic two-state N ⇌ S pseudorotational equilibrium2bg[3] of the β-D-pentofuranose moiety in adenosine 3′,5′-bisphosphate [EtpApMe (**1**)] and in its abasic counterpart [Etp(apurinic)pMe (**2**)] influenced by the steric and stereoelectronic forces depending upon the nature and relative orientation of various sugar substituents[2,3a]

of pH, compared with the complete absence of such effect in the apurinic counterpart [Etp(apurinic)pMe (**2**)]. It has been demonstrated that as the electronic character of adenine moiety in **1** changes as a function of change of the protonation ⇌ deprotonation equilibrium[2o] at N1, the strength of the anomeric effect ($n_{O4'} \rightarrow \sigma^*_{C1'—N9}$ orbital mixing [2l,m,o,3a,4,13]) is continuously modulated to induce a change in the electron density at O4′ (tunable $n_{O4'} \rightarrow \sigma^*_{C1'—N9}$ orbital mixing), which, in turn, dictates the nature of the orbital overlap of $\sigma_{C3'—H3'}$ with $\sigma^*_{C4'—O4'}$ as well as the stabilization energy of the newly formed hybrid orbitals (the 3′-*gauche* effect: $\sigma_{C3'—H3'} \rightarrow \sigma^*_{C4'—O4'}$ orbital mixing [2,13a,5,13]). The change of electron density at C3′ due to the effective interplay of the 3′-*gauche* effect further influences the electron density of O3′ and consequently the orbital overlap capability of its lone pair with the antibonding orbital of P3′— O(ester) [a tunable anomeric transmission of $n_{O3'} \rightarrow \sigma^*_{P3'—O(ester)}$]. This tunable transmission of the charge density from the aglycone, turning the conformational wheel across the sugar–phosphate backbone, is influenced by the relative donor–acceptor capabilities of bonding, non-bonding and antibonding orbitals of various sugar atoms and substituents, thereby tuning the electron-density potential of various donor and acceptor orbitals both by through-space and through-bond effects[13].

RESULTS AND DISCUSSION

The basis of our analysis is as follows. The mole fractions of N- and S-type conformers from pD 1.0 to 7.9 were calculated by the pseudorotational analysis[2,3a,6–8] (J. van Wijk, unpublished results) of temperature-dependent $3J_{HH}$ using the PSEUROT program (v. 5.4)[7] based on a generalized Karplus-type equation[8a,b] to give $\Delta G°$ of the two-state N ⇌ S pseudorotational equilibrium of the sugar moiety at each of the seven pDs ranging from 7.9 to 1.0 (Table 1). The pD values correspond to the reading on a pH meter with a calomel electrode, and are not

Table 1. Determination of pD-dependent $\Delta G°$ of two-state N ⇌ S and $\varepsilon^t \rightleftharpoons \varepsilon^-$ equilibrium from pseudorotational analyses and EPSILON calculation, respectively, at 298 K for EtpApMe (**1**)[a]

	N ⇌ S equilibrium		$\varepsilon^t \rightleftharpoons \varepsilon^-$ equilibrium	
pD	ΔG^{298} (σ)[b]	S(%)	ΔG^{298} (σ)[b]	ε^-(%)
1.0	−1.7(0.2)	67	−1.5(0.2)	65
2.0	−2.0(0.2)	69	−1.6(0.2)	66
2.5	−2.0(0.2)	69	−1.6(0.2)	66
3.0	−2.1(0.2)	70	−1.6(0.2)	66
3.5	−2.2(0.2)	71	−1.7(0.2)	66
4.0	−2.4(0.2)	73	−1.8(0.2)	67
4.5	−2.7(0.2)	75	−1.9(0.2)	68
4.8[c]	−2.8(0.2)	—	−2.0(0.2)	—
7.9	−2.8(0.2)	76	−1.9(0.1)	68

[a]For the experimental procedure used to calculate the values see the supporting information.
[b]ΔG^{298} in kJ mol^{-1} of N ⇌ S and $\varepsilon^t \rightleftharpoons \varepsilon^-$ equilibrium was calculated directly from the average logarithm $\ln_{av}[x_a/(1-x_a)]$ by using the Gibbs equation, $\Delta G^T = -(RT/1000)\ln_{av}[x_a/(1-x_a)]$ with $1-x_a = x_b$, where $x_a = x_S$ or x_{ε^-} and $x_b = x_N$ or x_{ε^t}, respectively, and R is the gas constant and T is the absolute temperature. Standard deviations are given in parentheses.
[c]Owing to the overlapping of H2′ and H3′ peaks with the residual water signal at 298 K for pD = 4.8, the coupling values could not be used in any conformational analyses, so in order to calculate ΔG^{298} the value of $\ln_{av}[x_a/(1-x_a)]$ at pD 4.8 was extrapolated.

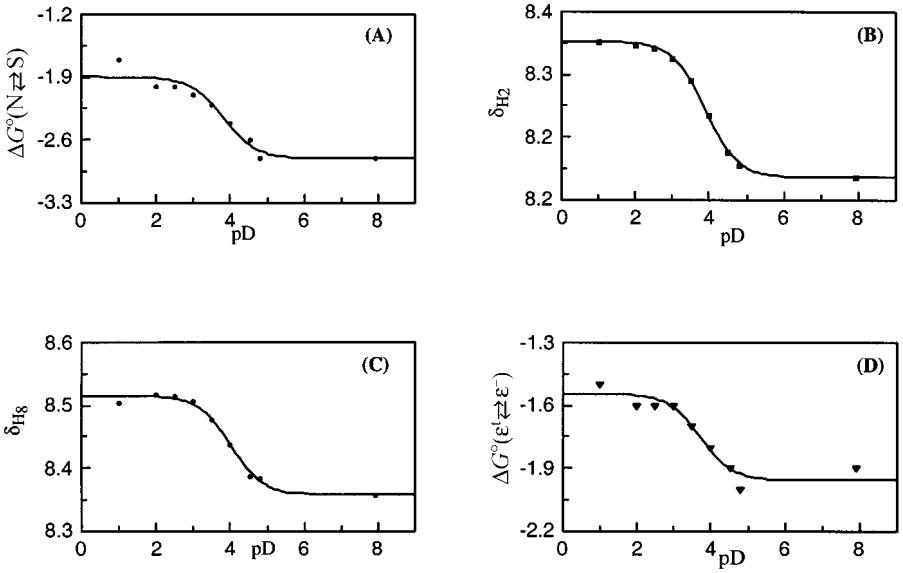

Figure 2. Plots of H2 chemical shift (δ H2 in ppm) (B) and H8 chemical shift (δH8 in ppm) (C) of the constituent adenin-9-yl nucleobase, the experimental $\Delta G°$ (kJ mol^{-1}) of the N $\rightleftharpoons$ S pseudorotational equilibrium of the constituent pentofuranse moiety (A) and $\Delta G°$ (kJ mol^{-1}) of the $\varepsilon^t \rightleftharpoons \varepsilon^-$ equilibrium (D) of the constituent 3′-ethylphosphate group in EtpApMe (**1**) as a function of pD at 298K, showing sigmoidal curves. The sigmoidal curves are the result of the best iterative least-squares fit of the pD-dependent (i.e. nine pDs in the range 1.0–7.9) δH2 (B), δH8 (C), the experimental $\Delta G°$ values of the N $\rightleftharpoons$ S equilibrium (A) and the experimental $\Delta G°$ values of the $\varepsilon^t \rightleftharpoons \varepsilon^-$ equilibrium (D) to the Henderson–Hasselbach equation (see Experimental section for details). The following values for the pD at the inflection point of each plot were obtained from this least-squares fit: 3.8 (A), 3.9 (B), 4.0 (C) and 3.7 (D); these values (within the range of our experimental error, $\pm$0.3 unit) were verified using corresponding Hill plots (Fig. S1 in the supporting information)

corrected for the deuterium isotope effect. As the medium becomes more acidic, N1 of adenin-9-yl becomes protonated[2o,] and the electron density at N9 is reduced owing to the drainage of charge density from the electron-rich imidazole to the electron-deficient pyrimidine part, causing an increase in the strength of the anomeric effect [$n_{O4'} \rightarrow \sigma^*_{C1'—N9}$ orbital mixing][2l,m,o]. The conformational outcome of this is that the aglycone takes up the pseudoaxial orientation and the N $\rightleftharpoons$ S pseudorotational equilibrium for EtpApMe (**1**) is gradually shifted towards N-type (from 76% S at pD 7.9 to 67% S at pD 1.0), which is reflected from the change of $\Delta G°$ (at 298 K) from -2.8 kJ mol^{-1} at pD 7.9 to -1.7 kJ mol^{-1} at pD 1.0 (Table 1).

The plot of pD-dependent $\Delta G°$ values[2l,n,o,q] of the N $\rightleftharpoons$ S equilibrium in EtpApMe (**1**) [in Fig. 2 (A) has the typical sigmoidal shape with a value of 3.8 at the inflection point which is identical with the pK_a of the constituent adenin-9-yl, determined independently from the plot of pD-dependent H2 and H8 chemical shifts [Fig. 2 (B)]. The pK_a value for EtpApMe (**1**) was confirmed by the Hill plot[2l,n,o,q] (Fig. S1 in the supporting information) showing the characteristics of a single protonation site. As a control experiment, the difference in $3J_{HH}$ values between neutral and acidic pDs at 298 K (Table S5 in the supporting information) was found to be negligible ($\pm$0.1 Hz over the whole pD range studied) in the apurinic phosphodiester **2**, showing that in the absence of the aglycone, its N $\rightleftharpoons$ S equilibrium is unbiased and remains unchanged at all pDs compared with **1**.

Since the ε^+ conformer across the C3′—O3′ bond is energetically forbidden,[9a] and is not found in the crystal data,[9b] the temperature-dependent $^3J_{C4',P3'}$, $^3J_{C2',P3'}$ and $^3J_{H3',P3'}$ experimental coupling constants for **1** have been interpreted in terms of a two-state $\varepsilon^t \rightleftharpoons \varepsilon^-$ equilibrium.[2k] The temperature-dependent mole fractions of the two-state $\varepsilon^t \rightleftharpoons \varepsilon^-$ equilibrium have been calculated using the program EPSILON2ek[9,10] (See supporting information for the experimental details). The logarithm of the ratio of the resulting mole fractions of ε^- and ε^t gave $\Delta G°$ at 298 K for the $\varepsilon^t \rightleftharpoons \varepsilon^-$ equilibrium for **1** at each of the seven pDs ranging from 7.9 to 1.0, varying from -1.9 to -1.5 kJ mol^{-1} (Table 1) for the population of ε^- (at 298 K) decreasing from 68% at pH 7.9 for neutral adenine to 65% at pH 1.0 for N1-protonated adenine. In the case of our reference apurinic phosphodiester **2**, no change in $^3J_{H,P}$ and $^3J_{C,P}$ coupling constant values was observed compared with that of purinic phophodiester **1** over the whole pD range (Table S4 in the supporting information), thereby allowing us to conclude that the conformational changes observed across C3′—O3′ in **1** over the whole pD range are a result of modulation of the electronic character from the neutral adenine moiety to adenine-N1H$^+$. Interestingly, the plot of pD-dependent $\Delta G°$ values of the $\varepsilon^t \rightleftharpoons \varepsilon^-$ equilibrium in EtpApMe **1** also gives a sigmoidal curve Fig. 2 (D), just as found for the

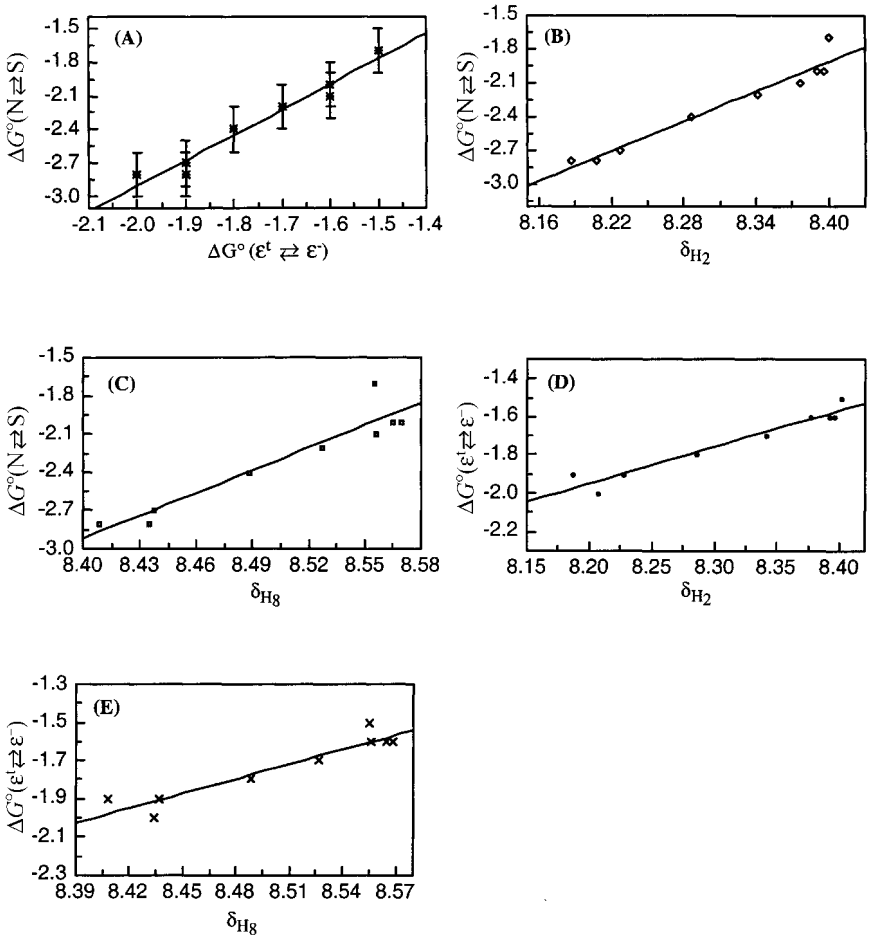

Figure 3. . (A) Plot of $\Delta G°$ (kJ mol^{-1}) of the N ⇌ S pseudorotational equilibrium at 298 K in **1** as a function of $\Delta G°$ (kJ mol^{-1}) of its $\varepsilon^t \rightleftharpoons \varepsilon^-$ equilibrium at nine pD values ranging from 1.0 to 7.9 showing a straight line ($R = 0.98$) with a slope of 2.25 ($\sigma = 0.1$) and an intercept of 1.6 ($\sigma = 0.17$). The vertical bars show the standard deviations ($\sigma = 0.2$) at each pD. (B) Plot of $\Delta G°$ (kJ mol^{-1}) of the N ⇌ S pseudorotational equilibrium in **1** as a function of δH2 (ppm) of the constituent adenin-9-yl at 298 K at nine different pD values ranging from 1.0 to 7.9 showing a straight line ($R = 0.98$) with a slope 4.37 ($\sigma = 0.24$) and an intercept of -38.62 ($\sigma = 1.97$). (C) Plot of $\Delta G°$ (kJ mol^{-1}) of the N ⇌ S pseudorotational equilibrium in **1** as a function of δH8 (ppm) of the constituent adenin-9-yl at 298 K at nine different pD values ranging from 1.0 to 7.9 showing a straight line ($R = 0.95$) with a slope of 5.90 ($\sigma = 0.44$) and an intercept of -52.46 ($\sigma = 3.76$). (D) Plot of $\Delta G°$ (kJ mol^{-1}) of the $\varepsilon^t \rightleftharpoons \varepsilon^-$ equilibrium in **1** as a function of δH8 (ppm) of its adenin-9-yl at 298 K at nine different pD values ranging from 1.0 to 6.7, showing a straight line ($R = 0.97$) with a slope of 1.89 ($\sigma = 0.12$) and an intercept of -17.46 ($\sigma = 0.97$). (E) Plot of $\Delta G°$ (kJ mol^{-1}) of the $\varepsilon^t \rightleftharpoons \varepsilon^-$ equilibrium in **1** as a function of δH8 (ppm) of the constituent adenin-9-yl at 298 K at nine different pD values ranging from 1.0 to 7.9 showing a straight line ($R = 0.94$) with a slope of 2.55 ($\sigma = 0.21$) and an intercept of -23.44 ($\sigma = 1.76$)

plot of the corresponding pD-dependent $\Delta G°$ values of the N ⇌ S equilibrium of the constituent pentofuranose sugar Fig. 2 (A). The value of pD (i.e. pD = 3.7) at the inflection point of the graph shown in Fig. 2(D) is nearly identical (i.e. within the accuracy of the measurements, ± 0.1 Hz) with the pK_a values of the adenin-9-yl obtained by pD-dependent plot of δH2 (pK_a = 3.9) and δH8 (pK_a = 4.0) in EtpApMe **1**, which were also conformed by the Hill plot analysis[2l,n,o,q] (Fig. S1 in the supporting information). Thus, the pD-dependent conformational reorientation of the C3′—O3′ bond (reflected in $\Delta G°$ values of the $\varepsilon^t \rightleftharpoons \varepsilon^-$ equilibrium) is directly dictated by the electronic character of the constituent C1′-aglycone in EtpApMe **1**.

The correlation plot of pD-dependent $\Delta G°$ values of the N ⇌ S equilibrium of the pentofuranose sugar as a function of pD-dependent $\Delta G°$ values of the $\varepsilon^t \rightleftharpoons \varepsilon^-$ equilibrium of the 3′-phosphate moiety in **1** gives a straight line with a high Pearson correlation coefficient [$R = 0.98$, Fig. 3(A)]. This indicates that as the constituent adenin-9-yl nucleobase in **1** becomes gradually protonated in the acidic medium, the modulation of the strength of the anomeric effect shifts the N ⇌ S equilibrium toward N, which in turn dynamically shifts the $\varepsilon^t \rightleftharpoons \varepsilon^-$ equilibrium toward ε^t in comparison with the neutral pD. Other important items of evidence for the transmission of the free energy of the protonation–deprotonation equilibrium of the nucleobase steering the

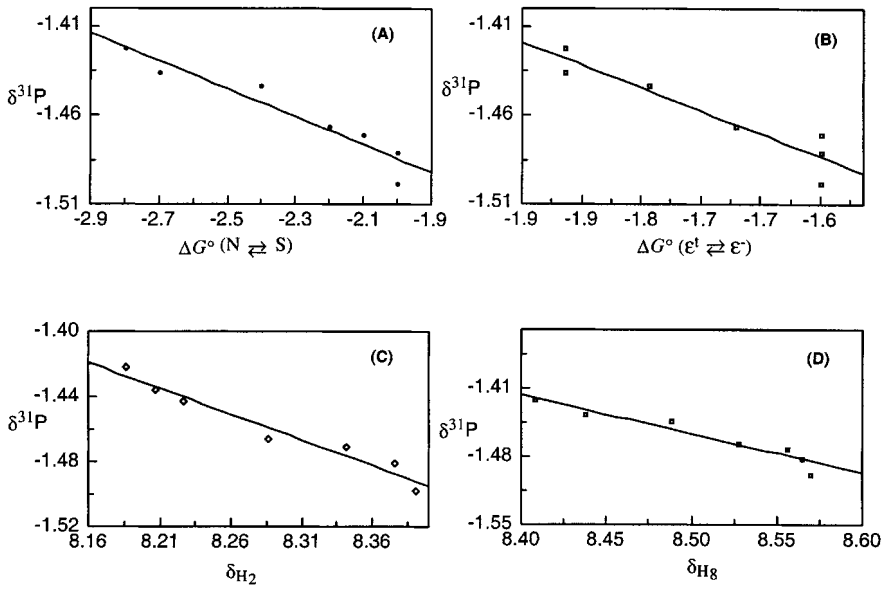

Figure 4. . (A) Plot of ^{31}P chemical shift of P3 (δ^{31}P in ppm) of EtpApMe (**1**) as function of $\Delta G°$ (kJ mol^{-1}) of the N ⇌ S pseudorotational equilibrium at seven pD values ranging from 2.0 to 7.9 showing a straight line ($R = 0.97$) with a slope of -0.08 ($\sigma = 0.01$) and an intercept of -1.64 ($\sigma = 0.02$). (B) Plot of δ^{31}P in EtpApMe (**1**) as a function of $\Delta G°$ (kJ mol^{-1}) of the $\varepsilon^t \rightleftharpoons \varepsilon^-$ equilibrium at seven pD values ranging from 2.0 to 7.9 showing a straight line ($R = 0.94$) with a slope of -0.19 ($\sigma = 0.01$) and an intercept of -1.77 ($\sigma = 0.02$). (C) Plot of δ^{31}P in EtpApMe (**1**) as a function of δH2 of its adenin-9yl at 298 K at seven pD values ranging from 2.0 to 7.9 showing a straight line (R = 0.96) with a slope of -0.32 ($\sigma = 0.02$) and an intercept of 1.15 ($\sigma = 0.15$). (D) Plot δ^{31}P in EtpApMe (**1**) as a function of δH8 of its adenin-9-yl at 298 K at seven pD values ranging from 2.0 to 7.9 showing a straight line ($R = 0.96$) with a slope of -0.40 ($\sigma = 0.03$) and an intercept of -1.93 ($\sigma = 0.27$)

phosphate conformation through the change of the conformation of the sugar moiety are the correlation plots of pD-dependent H2 or H8 proton chemical shifts as a function of (i) the pD-dependent $\Delta G°$ values of the N ⇌ S equilibrium [Fig. 3(B) and (C)], (ii) the pD-dependent $\Delta G°$ values of the $\varepsilon^t \rightleftharpoons \varepsilon^-$ equilibrium [Fig. 3(D) and (E)] or (iii) the pD-dependent ^{31}P chemical shift of 3′-phosphate [Fig. 4(C) and (D)] in **1**, all of which give straight lines with high correlation coefficients ($R = 0.98$, 0.95, 0.97, 0.94, 0.96 and 0.96, respectively). In addition, the plots of pD-dependent ^{31}P chemical shift of 3′-phosphate either as a function of pD-dependent $\Delta G°$ values of the N ⇌ S equilibrium [$R = 0.97$; Fig. 4(A)] or as a function of pD-dependent $\Delta G°$ values of the $\varepsilon^t \rightleftharpoons \varepsilon^-$ conformational equilibrium [$R = 0.94$; Fig. 4(B)] also give straight correlations, suggesting that the sugar–phosphate backbone conformation dictates the ^{31}P chemical shift of the 3′ -phosphate moiety in **1**.

Consistent with our earlier observations on ribonucleoside 3′-ethylphosphates[2k] at neutral pH at room temperature, we found non-equivalence of methylene protons of the 3′ -ethyphosphate moiety in **1** owing to the 2′ -OH-promoted hydrogen bonding with the vicinal O3′. Hence all our temperature-dependent $\Delta G°$ measurements were performed well below the hydrogen-bond melting temperature (i.e. 298 K) for **1** over the whole pH range (1.0–7.9). This means that all changes of free energy observed at 298 K (Table 1) for **1** as the pH changes are attributed to the free-energy changes of the protonation–deprotonation equilibrium of the aglycone to drive the sugar–phosphate backbone in a concerted manner.

The proof of the one-way transmission of stereoelectronic information in EtpApMe **1** from the aglycone to the sugar to the phosphate are twofold. (1) The pK_a value of the adenin-9-yl aglycone remains very close to 3.8, being independent of any OH or phosphate substituents in the sugar moiety. Thus the pK_a values of N1 of the adenin-9-yl moiety in the following series of adenine nucleosides are as follows within the error limits of our NMR experiments:[2] 2′,3′ -dideoxyadenosine (pK_a 3.8), 2′ -deoxyadenosine (pK_a 3.5), adenosine (pK_a 3.5) and EtpApMe **1** [(pK_a 3.9 (from H2 chemical shift), pK_a 4.0 (from H8 chemical shift)]. (2) When the 3′ -phosphate (p$K_a \approx 1.5$) in Etp(apurinic)pMe **2** becomes partially protonated at pD 1.6 under our experimental conditions, the endocyclic sugar $^3J_{HH}$ remains unaltered (Table S5 in the supporting information) compared with EtpApMe **1** (Table S3 in the supporting information), suggesting that a change in the electronic character of the phosphate does not influence the structural and dynamic character of the sugar moiety.

CONCLUSION

As the pD-tunable change of the electronic character of

the nucleobase tunes the strength of the anomeric effect, an increased preference of the N-type sugar conformation is imposed because of enhanced $n_{O4'} \rightarrow \sigma^*_{C1'—N9}$ orbital mixing,[2lmo3a,4,13,14] which in turn affects the strength of the [O3′—C3′—C4′—O4′] *gauche* effect by retuning the energy levels of the donor and acceptor orbitals in the $\sigma_{C3'—H3'} \rightarrow \sigma^*_{C4'—O4'}$ interaction.2l3a[5,13] The extent of $\sigma_{C3'—H3'} \rightarrow \sigma^*_{C4'—O4'}$ participation influences the electron density at O3′, which in turn modulates the O3′—P3′—O anomeric effect[3a] (Ref. 11 for the anomeric effect across the 3′ O—P—O— ester fragment in the sugar–phosphate backbone) [a tunable transmission of $n_{O3'} \rightarrow \sigma^*_{P3'—O(ester)}$ orbital interaction].[13] Hence this interplay of the stereoelectronic *gauche* and anomeric effects defines the overall conformation of the ubiquitous adenine ribonucleotide, thereby contributing to the stability of the three-dimensional structure of the RNA besides H-bonding, stacking, intermolecular electrostatic interactions and hydration.

EXPERIMENTAL

All experimental details are given in the supporting information, available on the epoc website, which contains the following:

1. Tables S1–S3 and S5 contain information on chemical shift and coupling constant changes at nine different pDs (1.0–7.9) at room temperature and two extreme temperatures.
2. Pseudorotational analysis of the coupling constants using the PSEUROT program at various pDs (Table S4), including the coupling constant fitting process with the conformational hyperspace.
3. Crystal data analysis of various forms of RNA to calculate the average ε values (Table S6).
4. Estimation of epsilon rotamers using the EPSILON program.
5. Hill plots for pK_a determination (Fig. S1).
6. Synthesis of adenosine 3′,5′-bisphosphate [EtpApMe (**1**)] and its apurinic counterpart of adenosine 3′,5′-bisphosphate [Etp(apurinic)pMe (**2**)].

Acknowledgements

We thank the Swedish Board for Technical Development (TFR), the Swedish Natural Science Research (NFR) Council and the Swedish Board for Technical Development (NUTEK) for generous financial support. Thanks are due to the Wallenbergstiftelsen, Forskningsrå dsnämnden and University of Uppsala for funds for the purchase of 500 and 600 MHz Bruker DRX NMR spectrometers.

REFERENCES

1. (a) Saenger W. *Principles of Nucleic Acid Structure*. Springer: Berlin, 1998; (b) Peter RE, Dandliker J, Barton JK. *Angew. Chem. Int. Ed. Engl*. 1997; **36**: 2714; (c) Meggers E, Kusch D, Spichty M, Wille U, Giese B. *Angew. Chem. Int. Ed. Engl.* 1998; **37**: 460.
2. (a) Koole LH, Buck HM, Nyilas A, Chattopadhyaya J. *Can J. Chem.*, 1987; **65**: 2089; (b) Plavec J, Koole LH, Chattopadhyaya J. *J. Biochem. Biophys. Methods* 1992; **25**: 253; (c) Plavec J, Garg N, Chattopadhyaya J. *J. Chem. Soc., Chem. Commun.* 1993; 1011; (d) Plavec J, Tong W, Chattopadhyaya J. *J. Am. Chem. Soc.* 1993; **115**: 9734; (e) Plavec J, Thibaudeau C, Viswanadham G, Sund C, Chattopadhyaya J. *J. Chem. Soc., Chem. Commun.* 1994; 781 (f) Thibaudeau C, Plavec J, Garg N, Papchikhin A, Chattopadhyaya J. *J. Am. Chem. Soc.* 1994; **116**: 4038; (g) Plavec J, Thibaudeau C, Chattopadhyaya J. *J. Am. Chem. Soc*. 1994; **116**: 6558; (h) Plavec J, Thibaudeau C, Chattopadhyaya J. *J Am. Chem. Soc.* 1994; **116**: 6558; (i) Thibaudeau C, Plavec J, Watanabe KA, Chattopadhyaya J. *J. Chem. Soc., Chem. Commun.* 1994; 537; (j) Thibaudeau C, Plavec J, Chattopadhyaya J. *J. Am. Chem. Soc.* 1994; **116**: 8033; (k) Plavec J, Thibaudeau C, Viswanadham G, Sund C, Sandstrom A, Chattopadhyaya J. *Tetrahedron* 1995; **51**: 11775, and references cited therein; (l) Thibaudeau C, Plavec J, Chattopadhyaya J. *J. Org. Chem.* 1996; **61**: 266; (m) Plavec J, Thibaudeau C, Chattopadhyaya J. *Pure Appl. Chem.* 1996; **68**: 2137; (n) Thibaudeau C, Földesi A, Chattopadhyaya J. *Tetrahedron* 1997; **53**: 14043; (o) Luyten I, Thibaudeau C, Chattopadhyaya J. *J. Org. Chem.* 1997; **62**: 8800; (p) Thibaudeau C, Földesi A, Chattopadhyaya J. *Tetrahedron* 1998; **54**: 1867; (q) Luyten I, Thibaudeau C, Chattopadhyaya J. *Tetrahedron* 1997; **53**: 6433; (r) Thibaudeau C, Plavec J, Chattopadhyaya J. *J. Org. Chem.* 1998; **63**: 4967.
3. (a) For review, see Thibaudeau C, Chattopadhyaya J. *Stereoelectronic Effects in Nucleosides and Nucleotides and their Structural Implications*. Uppsala University Press: Uppsala, 1999; (b) de Leeuw HPM, Haasnoot CAG, Altona C. *Isr. J. Chem.* 1980; **20**: 108.
4. (a) Petillo PA, Lerner LA. In *The Anomeric Effect and Associated Stereoelectronic Effects*, Thatcher GRJ (ed). *ACS Symposium Series*. American Chemical Society: Washington, DC, 1993; 156, and references cited therein; (b) Perrin CL, Armstrong KB, Fabian MA. *J. Am. Chem. Soc.* 1994; **116**: 715.
5. (a) Dionne P, St-Jacques M. *J. Am. Chem. Soc.* 1987; **109**: 2616; (b) Wiberg KB. *Acc. Chem. Res.* 1996; **29**, 229, and references cited therein.
6. (a) Altona C, Sundaralingam M. *J. Am. Chem. Soc.* 1972; **94**: 8205; (b) Altona C, Sundaralingam M. *J. Am. Chem. Soc.* 1973; **95**: 2333.
7. (a) De Leeuw FAAM, Altona C. *J. Comput. Chem.* 1983; **4**: 428; PSEUROT, QCPE Program No. 463; (b) Haasnoot CAG, de Leeuw FAAM, Altona C. *Tetrahedron* 1980; **36**: 2783.
8. (a) Diez E, Fabian JS, Guilleme J, Altona C, Donders LA. *Mol. Phys.* 1989; **68**: 49; (b) Donders LA, de Leeuw FAAM, Altona C. *Magn. Reson. Chem.* 1989; **27**: 556; (c) Altona C, Ippel JH, Hoekzema AJAW, Erkelens C, Groesbeek G, Donders LA. *Magn. Reson. Chem.* 1989; **27**: 564.
9. (a) Dhingra MM, Saran A. *Bioploymers* 1982; **21**: 859; (b) Lankhorst PP, Haasnoot CAG, Erkelens C, Altona C. *J. Biomol. Struct. Dyn.* 1984; **1**: 13870; (c) Blommers MJJ, Nanz D, Zerbe O. *J. Biomol. NMR* 1994; **4**: 595.
10. (a) Press WH, Flannery BP, Tenkolsky SA, Vatterling WT. *Numerical Recipes (Fortran Version)*. Cambridge University Press: New York, 1999; (b) Mooren MMW, Wijmenga SS, van der Marel GA, van Boom JH, Hilbers CW. *Nucleic Acids Res.* 1994; **22**: 2658; (c) Plavec J, Chattopadhyaya J. *Tetrahedron* 1995; **36**: 1949.
11. Saenger W. *Principles of Nucleic Acid Structure*. Springer: Berlin, 1988; 93–96, and references cited therein.
12. (a) Haasnoot CAG, de Leeuw FAAM, de Leeuw HPM, Altona C. *Recl. Trav. Chim. Pays-Bas* 1979; **98**: 576; (b) Rosemeyer H, Tóth G, Golankiewicz B, Kazimierczuk Z, Bourgeois W, Kretschmer U, Muth HP, Seela F. *J. Org. Chem.* 1990; **55**: 5784.
13. Acharya P, Trifonova A, Thibaudeau C, Földesi A, Chattopadhyaya J. *Angew. Chem. Int. Ed. Engl.* 1999; **38**: 3645.
14. Polak M, Plavec J, Trifonova A, Földesi CA, Chattopadhyaya J. *J. Chem. Soc. Perkin Trans.* 1999; **1**: 2835.